THE ASTROPHYSICAL JOURNAL, 327:116–127, 1988 April 1

THICK ACCRETION DISKS AROUND BLACK HOLES AND THE UV/SOFT X-RAY EXCESS IN QUASARS

PIERO MADAU
International School for Advanced Studies, SISSA, Trieste
Received 1987 April 14; accepted 1987 September 25

ABSTRACT

The optical/UV bump seen in quasars is often modeled as the integrated thermal emission from an optically thick, geometrically thin accretion disk around a supermassive black hole. Soft X-ray excesses recently detected in optically selected (PG) quasars have consequently been attributed to the hot tail of the accretion disk spectrum. However, the high temperatures and luminosities inferred favor a picture in which supercritical, radiation-supported tori around 10^7–10^8 $M_\odot$ black holes are responsible for the UV/soft X-ray thermal component.

We investigate models of thick accretion disks and, in particular, the effects of the toroidal shape on the observed thermal emission. The occultation of the innermost disk region due to self-shadowing and the reflection effect of photons off the funnel walls are taken into account. The dependence of the observed spectrum on the viewing angle is discussed. It is suggested that high- and low-inclination systems are responsible for the optical/UV and UV/soft X-ray excesses, respectively.

Subject headings: black holes — quasars — radiation mechanisms — stars: accretion

I. INTRODUCTION

The 10–0.1 μm continuum of quasars and Seyfert galaxies can be decomposed into a single power law $F_\nu \propto \nu^{-\alpha}$ (with $\alpha \approx 1$) plus a superposed "bump" in the blue and near-UV band (Neugebauer *et al.* 1979; Richstone and Schmidt 1980).

This optical/UV excess above the extrapolated nonthermal IR continuum has been attributed by Shields (1978) and later by Malkan and Sargent (1982) to a thermal component peaking at ultraviolet frequencies and approximately described by a single-temperature blackbody with $T \approx 30{,}000$ K. This component flattens the quasar continuum starting at around ~ 5000 Å; the optical/UV spectra would then steepen at wavelengths shorter than ~ 1500 Å because of the exponential cutoff of this thermal component.

It is now widely believed that accretion onto supermassive black holes is the power source for active galactic nuclei (see Rees 1984 for a recent review). Material with specific angular momentum exceeding $3^{1/2} r_G c$ (with $r_G = 2GM/c^2$ for a Schwarzschild black hole of mass M) cannot be accreted directly and settles down into a disk.

Different regimes of accretion with angular momentum have been distinguished, depending on the ratio, $\dot{m}$, of the accretion rate, $\dot{M}$, to the Eddington accretion rate, $\dot{M}_E = L_E/c^2 = 4\pi GM/(ck_T)$, where k_T is the relevant opacity (Thomson in this case) and L_E is the Eddington limit (see, e.g., Blandford 1984; Begelman 1985; and references therein).

Much interpretative work has been devoted to geometrically thin disks accreting mass at a subcritical rate, i.e., $\dot{m} \ll 10$ (for a review, see Pringle 1981). Thin Keplerian disks can efficiently cool on the infall time scale; they are thermal, broad-band emitters, the spectrum reflecting the radial variation of the disk surface temperature.

In the blackbody approximation, the maximum temperature

$$T_{\max} \approx 6 \times 10^4 \dot{m}^{1/4} M_8^{-1/4} \qquad (1)$$

is achieved at $r \approx 5r_G$, where M_8 is the mass of the hole in 10^8 solar mass units. The emitted spectrum peaks in the near-UV band, so it was natural to interpret the UV bump seen in quasars as the integrated thermal emission from an accretion disk around a $\sim 10^8$ $M_\odot$ black hole (Shields 1978; Malkan 1983).

Spectral fits with accretion disk models have been performed by Malkan (1983). The single blackbody fits of the *IUE* spectra of high-z QSOs apparently seem to have too little flux at the highest frequencies. A broader spectral distribution than a single Planck function, such as a sum-of-blackbodies accretion disk spectrum, seems to improve the fit.

It has been recently shown by Elvis *et al.* (1986) that a single power-law of slope $\alpha \sim 1$ could cover five decades of frequencies from IR to X-ray in optically selected (PG) quasars, with the UV thermal component forming a bump on top of it. However, in at least one object, the quasar PG 1211+143, a soft X-ray excess has been detected at energies ≤ 1 keV (Elvis, Wilkes, and Tananbaum 1985).

If thermal in origin, this excess would naturally be connected with the UV bump and interpreted as the hot tail of a single, very luminous thermal component with a much higher peak temperature $T_{\max} \approx 0.5$–1×10^6 K. More recently, other examples of quasars with soft X-ray excesses have been reported (Singh, Garmire, and Nousek 1985; Arnaud *et al.* 1985; Pounds *et al.* 1986).

Observations of the maximum temperature $T_{\max}$ are then of great importance for disk models, because it constrains the mass and the accretion rate of the central engine. Thin disk model fits of the UV/soft X-ray excesses require $L \gg L_E$ or, equivalently, $\dot{m} \gg 10$ (Bechtold *et al.* 1987).

The sum-of-blackbodies approximation on which these fits are based is somewhat doubtful. Opacity effects in thin accretion disks are very important; in the inner regions the electron scattering opacity will strongly modify the blackbody spectrum. At high accretion rates ($\dot{m} \geq 1$), the diffusion approximation is no longer valid and Comptonization may play a relevant role in the formation of the spectrum.

Modifications of the disk spectrum due to opacity effects require higher temperatures to radiate the same luminosity;

hence, soft X-ray excesses may be produced at much lower accretion rates. However, accretion rates which exceed the Eddington one, $\dot{m} \geq 10$, are still needed (Czerny and Elvis 1987). In this regime, where radiation pressure is dynamically important and the rotation law is no longer Keplerian, the standard theory of the thin disk is no longer appropriate. Under these conditions, it is expected that the disk will no longer be thin, but will rather puff up to form a *thick radiation-supported torus.*

Thick accretion disks have been actively investigated over the past few years (see, e.g., Maraschi, Reina, and Treves 1976; Kozlowski, Jaroszynski, and Abramowicz 1978; Frank 1979; Jaroszynski, Abramowicz, and Paczyński 1980; Paczyński and Wiita 1980). It is now well established that a major fraction of their liminosity is radiated from the surface of a funnel surrounding the rotation axis. In this region pressure gradients are balanced by centrifugal forces rather than by gravity; that is why the luminosities of such tori may well exceed the Eddington limit by large factors (Abramowicz, Calvani, and Nobili 1980). In the most extreme models studied so far, the high radiation flux density in the narrow funnel may accelerate matter in collimated jets (Abramowicz and Piran 1980). However, very little work has been done to express the theory of thick accretion disks in a form suitable for observational scrutiny. Instead, general theoretical arguments have been used to place self-consistency constraints on the models, but these still leave a wide range of possible configurations.

The very viability of some thick disk models has recently been put in question by the discovery (Papaloizou and Pringle 1984, 1985) that differentially rotating tori are subject to global, nonaxisymmetric dynamical instabilities. Work on understanding the physical causes of the instability has been limited to geometrically simple configurations, in particular slender tori and two-dimensional annuli (see Blaes 1986 and references therein). In the linear regime it is found that the quickest and most violent unstable modes are stabilized by steep angular momentum gradients (Goldreich, Goodman, and Narayan 1986). Recent nonlinear calculations by Blaes and Hawley (1987) show that the angular momentum redistribution which is driven by the instability results in configurations which can be characterized by a power-law angular momentum distribution (see also Zurek and Benz 1986). Disks with greater radial thickness saturate with flatter rotation laws. Moreover, disks with inner edges that overflow the potential cusp are quickly stabilized by the accretion flow (Blaes 1987).

An important feature of geometrically and optically thick disks is then investigated in this paper, namely the dependence of the observed disk spectrum on the viewing angle. Due to the doughnut shape, occultation of the innermost parts of the torus, which are found to be responsible for the emission in the soft X-ray band, occurs at large angles between the rotation axis and the line of sight.

It is found that the inner, very hot and luminous, funnel-shaped region dominates the emission from tori which are viewed more *pole-on*, i.e., at small viewing angles from the symmetry axis of the torus. This gives rise to a UV/soft X-ray thermal component such as that seen, e.g., in the quasar PG 1211+143. On the other hand, tori viewed nearly *edge-on*, i.e., at large viewing angles from the symmetry axis, appear less luminous and cooler, possibly accounting for the optical/UV bump.

In § II, a model of radiation-supported thick disks is analyzed. In § III the emitted spectrum is computed as a function of the inclination angle. The radiation field along the rotation axis is greatly enhanced by the multiple scatterings of photons off the funnel walls. This *reflection effect* is discussed in § IV. In § V we summarize our results and discuss them.

II. THE MODEL

The shape and structure of low-viscosity, non–self-gravitating thick accretion disks which are in hydrostatic equilibrium beyond their inner radii have been computed by several authors under a number of simplifying assumptions (see, e.g., Jaroszynski, Abramowicz, and Paczyński 1980; Paczyński and Wiita 1980). In the following, we shall consider such a torus as a toroidal, isolated star supported by radiation pressure, which is in pure rotation in the gravitational field of the black hole.

We adopt a cylindrical coordinate system (r, z, φ) centered on the hole. Further, we use here a pseudo-Newtonian potential of the form:

$$\phi = -GM/(R - r_G) , \qquad (2)$$

where $R = (r^2 + z^2)^{1/2}$ is the spherical radius. The self-gravity of the torus is taken to be negligible (this assumption will be checked *a posteriori*). It has been pointed out by Paczyński and Wiita (1980) that an ad hoc potential of this form mimicks the essential features of a Schwarzschild spacetime with regard to accretion flows. In particular, Keplerian orbits are bound if $r > 2r_G = r_{\rm mb}$, and stable if $r > 3r_G = r_{\rm ms}$; at $r_{\rm ms}$ we have the maximum binding energy and the minimum angular momentum.

The inner radius $r_{\rm in}$ of the torus lies between the marginally bound $r_{\rm mb}$ and marginally stable $r_{\rm ms}$ orbits; its location determines the efficiency ϵ of the conversion of accreted matter into radiation, i.e., $L = \epsilon \dot{M} c^2$. The maximum efficiency equals 6.25% at $r_{\rm ms}$, compared with the correct value 5.72% in the Schwarzschild case.

The shape and internal equilibrium structure of the rotating ring can be computed by assuming a barotropic equation of state $p = p(\rho)$. With this simplification, the specific angular momentum per unit mass $l(R)$ is constant on cylinders centered about the rotation axis and the hydrostatic equilibrium equation can be integrated to yield

$$\phi_{\rm eff}(r, z) = GM/(R - r_G) + \int (l^2/r^3) dr , \qquad (3)$$

where $\phi_{\rm eff}$ is the total (gravitational plus centrifugal) effective potential $\phi_{\rm eff} = \int dp/\rho$. Now, if one specifies *a priori* the rotation law $l(r)$, the shape of the equipotential surfaces can be determined. We take the boundary condition on the surface of the torus, defined by $h(r)$, to be the vanishing of the effective potential there. Then by specifying the inner edge $r_{\rm in}$ and the height at $r_{\rm in}$, the shape of the disk can be computed.

The acceptable forms of $l(r)$ are restricted by the requirements of local dynamical stability ($dl/dr \geq 0$) and inward accretion $[d/dr(lr^{-2}) < 0]$. Moreover, configurations with a flat distribution of angular momentum may be prone to global, nonaxisymmetric instabilities (Papaloizou and Pringle 1984). We will therefore consider a two-parameter angular momentum distribution:

$$l(r) = l_{\rm in}(r/r_{\rm in})^{2-q} ,$$

where $l_{\rm in}$ is the value of the Keplerian specific angular momentum at the inner edge $r_{\rm in}$. Rotation is Keplerian at the inner edge r_{in} of the torus and at the pressure maximum r_c located in the equatorial plane within a few gravitational radii. Inside r_c rotation is faster than the Keplerian one, and the excess centrifugal force is balanced by an inwardly directed pressure gradient.

Material is allowed to remain in stable circular orbits inside r_{ms} but outside the marginally bound orbit r_{mb}. However, for $r_{mb} \le r \le r_{ms}$, the binding energy, e, is reduced from its maximum value at r_{ms}, reaching zero at r_{mb}. In general, then, thick tori will be less efficient converters of rest mass to radiation than thin accretion disks.

A *cusp* forms at the inner radius r_{in}, i.e., a critical equipotential surface which crosses itself. If material fills this equipotential surface, the cusp will act as a Lagrangian point in a mass-transferring binary, and dynamical mass loss through the inner edge will take place. The assumption of hydrostatic equilibrium clearly breaks down close to the cusp, where a transition occurs from a subsonic inward drift to a supersonic, nearly radial free-fall.

Close to the rotation axis hydrostatic equilibrium is not possible; a hollow axial region or *funnel* forms, with its walls supported by centrifugal acceleration. Matter in the vortex funnel (which becomes a paraboloid for a flow with l = const) will either fall into the hole on a dynamical time scale or will be expelled to infinity by radiation pressure.

On the surface $h(r)$ we have $\phi_{eff} = 0$, and the shape of the torus is found to be

$$h(r) = \left\{\left[\frac{(r_{in} - r_G)Br_{in}^B - r_G(r^B - r_{in}^B)}{(r_{in} - r_G)Br_{in}^{B-1} - (r^B - r_{in}^B)}\right]^2 - r^2\right\}^{1/2} . \quad (4)$$

where $B = 2 - 2q$ and we have neglected the thickness of the flow at the inner radius. The outer radius r_{out} of the disk can be computed by solving $h(r_{out}) = 0$. Rather than assuming a value for the exponent q, one can equivalently specify the outer edge of the torus. The shape $h(r)$ will then be fully determined by specifying the inner and outer radii of our disk.

We assume a barotropic equation of state $p = K\rho^\gamma$, with K = const and $p = p_{gas} + p_{rad}$. If β denotes the ratio of gas pressure to total pressure, the distributions of density and temperature inside the torus are given by

$$\rho(r, z) = 4.82 \times 10^{12}[\beta^4/(1 - \beta)]\phi_{eff}^3(r, z) \text{ g cm}^{-3}$$

and

$$T(r, z) = 6.81 \times 10^{11}\beta\phi_{eff}(r, z) \text{ K} . \quad (5)$$

The assumption that the gravitational potential is determined by the central massive object is valid only if the total mass of the disk M_{disk} is less than the mass of the black hole M. The constraint $M_{disk} < M$ is found to be rather important in building self-consistent models (Abramowicz, Calvani, and Nobili 1980; Wiita 1982), actually providing more restrictions than the ones imposed by the onset of gravitational instabilities (which require the density in the disk at radius r to be much less than M/r^3; Paczyński 1978). The total mass of the disk, in units of $10^8 M_\odot$, is given by

$$M_{disk,8} = 7.85 \times 10^{12}M_8^3[\beta^4/(1 - \beta)] \int_{r_{in}}^{r_{out}} dr \int_0^{h(r)} \phi_{eff}^3(r, z)r\, dz . \quad (6)$$

The gas is taken to be fully ionized, with $\mu = \frac{1}{2}$. A sequence of barotropic models can now be constructed by varying the ratio, β, of the gas pressure to the total pressure. We assume β to be constant throughout the torus (see also Wiita 1982; Abramowicz, Henderson, and Ghosh 1983). Radiation-pressure support implies $\beta \ll 1$, subject to the constraints of self-consistency imposed by the conditions of hydrostatic equilibrium and negligible self-gravity.

Radiation-pressure support and electron scattering opacity allow us to compute the flux radiated from the known surface of the torus. If the disk atmosphere is in radiative and hydrostatic equilibrium, the critical flux emitted per unit area is

$$\boldsymbol{F}_r = -c/k_T \boldsymbol{g}_{eff} = -c/k_T(-\nabla\phi + \omega^2\boldsymbol{r}) , \quad (7)$$

where $\boldsymbol{g}_{eff}$ is the effective gravity vector (including the centrifugal force) which is perpendicular to the surface of the disk, and ω is the angular velocity.

The radial dependence of the effective temperature is given by:

$$\sigma T_{eff}^4(r) = \frac{c}{k_T}(1 - \beta)\left[\frac{G^2M^2}{(R - r_G)^4} + l^4r^{-6} - \frac{2GMl^2}{R(R - r_G)^2r^2}\right]^{1/2} , \quad (8)$$

where k_T is the Thomson opacity.

The total luminosity L is calculated by integrating equation (8) over the entire disk surface. It is possible to show that the ratio L/L_E is proportional to the logarithm of the ratio $Q = r_{out}/r_{in}$ (Abramowicz, Calvani, and Nobili 1980). For $Q > 50$, we derive

$$L/L_E \approx 3.8 \log Q - 2.43 . \quad (9)$$

As the inner radius cannot change by much ($2r_G \le r_{in} \le 3r_G$), it is the outer radius that really matters. Also, the structure of the disk at small radii is not sensitive to the disk structure at very large radii.

Within a thick torus there is no *local* energy balance because the generated heat can be transported both in the radial and in the vertical direction. However, there must be *global* mass, energy, and angular momentum conservation. To compute the luminosity generated in the torus we must integrate the total rate of dissipation in a cylindrical shell between the inner and outer radii, assuming dissipation and torques due to vertical shear to be negligible. The integration yields

$$L_g = \dot{M}[e_{in} - e_{out} - \omega_{out}(l_{out} - l_{in})] . \quad (10)$$

This formula is not symmetric with respect to the inner and outer edges because the torque at the inner edge vanishes, whereas it is nonzero at the outer edge. For large tori, $\omega_{out} l_{out} \to 0$ and $r_{out} \to 0$, and one has approximately that $L_g = \dot{M}e_{in}$. Of course, as $r_{in} \to r_{mb}$, $e_{in} \to 0$, and extremely large accretion rates are necessary to support a torus with a given luminosity.

At this point one generally assumes that there are no additional sources of energy (such as, e.g., nuclear burning), apart from viscous dissipation, and that negligible internal energy is advected in and out of the torus. In this case the local thin disk energy balance can be replaced by a global condition $L_g = L$ and we can solve equation (10) for the accretion rate $\dot{M}$. It turns out that, for a $\sim 10^8 M_\odot$ black hole, the thickness of the flow at r_{in}—and, consequently, the amount of internal energy swallowed by the hole—is small provided $\beta > 10^{-6}$ (Abramowicz 1985).

The knowledge of $\dot{M}$ allows us to give an *a posteriori* estimate of the kinematic viscosity, η, which is necessary to drive

TABLE 1

THE THICK ACCRETION DISK MODEL: CHARACTERISTIC VALUES

$L \approx 6L_E$
$\dot{M} \approx 20\ M_{\odot}\ \mathrm{yr}^{-1}$
$\epsilon \approx 6\%$
$\psi^a \approx 23°$
$M_{\mathrm{disk}} \approx 2.4 \times 10^6\ M_{\odot}$
$\alpha_c \approx 4. \times 10^{-7}$
$\rho_c \approx 2. \times 10^{-6}\ \mathrm{g\ cm^{-3}}$
$T_c \approx 7.6 \times 10^6$ K
Dynamical time scale at r_c: $t_d = 2\pi/\omega \approx 10^5$ s
Thermal time scale at r_c: $t_{\mathrm{th}} \approx t_d/\alpha \approx 10^4$ yr
Viscous time scale at r_c: $t_{\mathrm{vi}} \approx t_{\mathrm{th}}/(h/r)^2 \approx t_{\mathrm{th}}$

[a] $\psi \equiv$ half-opening angle of the funnel.

the accretion flow. Scaling η such that

$$\eta = \alpha^* \rho v_s H , \tag{11}$$

where v_s is the sound speed and H is the relevant length scale, the dimensionless viscosity parameter α^* can be computed (Wiita 1982).

Realistic thick accretion disks will resemble toroidal figures in dynamical equilibrium if the radial inward drift is dynamically unimportant, or, more in general, if departure from hydrostatic equilibrium is small. Because the disk is now geometrically thick, it is $(h/r) \approx 1$, and the condition of subsonic poloidal motion implies a tighter constraint on the magnitude of the viscosity: $\alpha^* \ll 1$ (Jaroszynski, Abramowicz, and Paczyński 1980).

III. THE SPECTRUM

A thick-disk model with parameters $r_{\mathrm{in}} = 2.7r_G$, $r_{\mathrm{out}} = 500r_G$, $M = 10^8\ M_{\odot}$, $\beta = 3 \times 10^{-4}$ is investigated in the rest of the article. The actual size of the disk is then $\sim 10^{16}$ cm, which is much smaller than the estimated radius, $\sim 10^{17}$ cm, of the broad emission line region in quasars (Gondhalekar, O'Brien, and Wilson 1986). Table 1 summarizes the relevant quantities of the model. The subscript "c" denotes values computed at the pressure maximum $r_c \approx 8r_G$. In a thick disk, most of the energy is released around r_c. The adopted value of the parameter β corresponds to a massive torus with a large optical depth. In this case the pressure scale height is much smaller than the disk thickness, and the atmosphere is very thin (Blandford 1985). The dimensionless accretion rate is $\dot{m} \approx 100$.

As electron scattering provides most of the opacity inside the torus, the emergent photons are thermalized on the surface where the effective absorption optical depth $\tau_* = [\tau_{\mathrm{ff}}(\tau_{\mathrm{ff}} + \tau_{\mathrm{T}})]^{1/2}$ is unity, τ_{T} and τ_{ff} being the electron scattering and free-free optical depth, respectively. For sufficiently high frequencies, scattering dominates free-free absorption and the photosphere lies well below the last scattering surface, as shown in Figure 1.

In Figure 2 the effective temperature distribution given by equation (8) is depicted. Similarly to what is found in thin disk models, the effective temperature has a sharp peak at a radius $r \approx 4r_G$, which is well inside the funnel. It then decreases roughly as $T_{\mathrm{eff}} \propto l^{1/2} r^{-3/4}$ in the region where the balance of forces is dominated by the centrifugal acceleration term, and

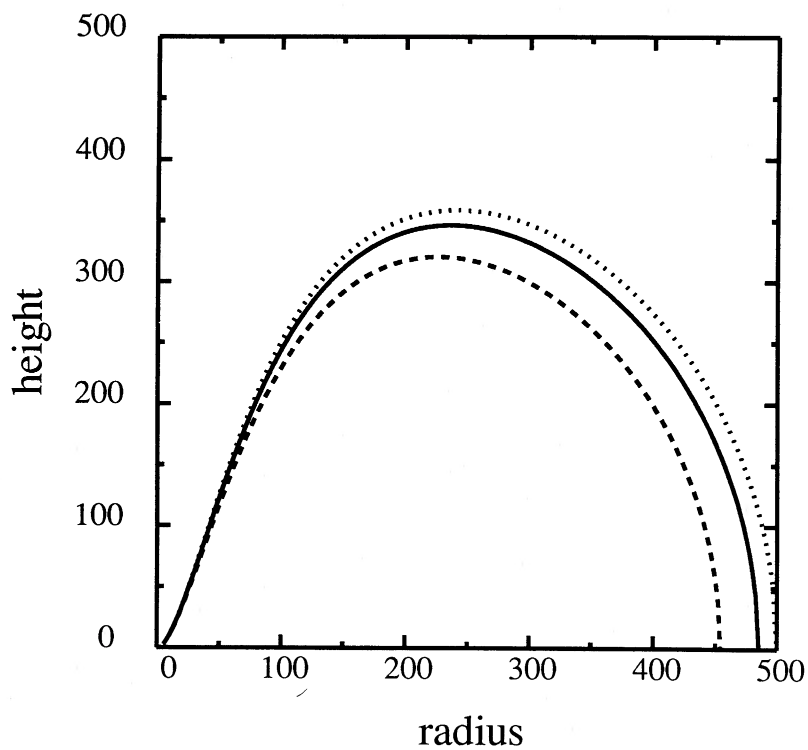

FIG. 1.—Meridional cross section of a radiation torus with model parameters: $r_{\mathrm{in}} = 2.7r_G$, $r_{\mathrm{out}} = 500r_G$, $M = 10^8\ M_{\odot}$, $\beta = 3 \times 10^{-4}$. The zero-pressure (*dotted curve*), last-scattering $\tau_{\mathrm{T}} = 1$ (*solid curve*), and thermalization $\tau_*(\nu) = 1$ for $\nu = kT/h$ (*dashed curve*) surfaces are plotted. Height and radius are in units of r_G. The optical depth is evaluated as $\tau = k\rho H$, where k is the specific opacity and H is the pressure scale height: $H = p/|\nabla p|$.

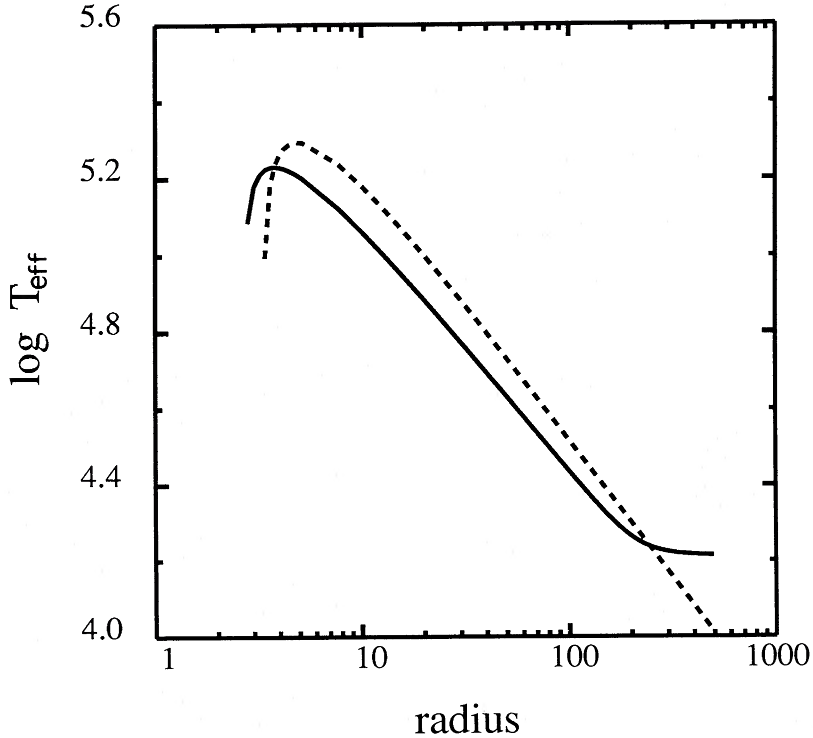

FIG. 2.—The effective temperature distributions for a radiation torus (*solid curve*) and for a thin accretion disk with the same values of M and $\dot{M}$ (*dashed curve*). The radius is in units of r_G. *Thin disk*: $T_{eff} \propto r^{-3/4}$; *radiation torus*: $T_{eff} \propto l^{1/2} r^{-3/4}$, where the centrifugal force dominates, and $T_{eff} \approx$ const where gravity dominates and the isobars are almost spherical.

finally becomes constant in the outer region, where pressure gradients balance against gravity and the isobars are almost spherical. For comparison purposes, the effective temperature distribution for a thin disk model with the same values of M and $\dot{M}$ is also shown.

To include the effect of Thomson opacity on the spectrum, a homogeneous, isothermal atmosphere is assumed here (Shakura and Sunyaev 1973). Then, since $k_T \gg k_{ff}(\nu)$, the emergent specific intensity (erg cm^{-2} s^{-1} Hz^{-1} sr^{-1}) is given by:

$$I_\nu = 3.2 \times 10^{-15} T_s^{11/4} [\beta/(1-\beta)]^{1/2} x^{3/2} e^{-x} (1 - e^{-x})^{-1/2} , \tag{12}$$

where $x = h\nu/kT_s$. The total modified blackbody flux (ergs cm^{-2} s^{-1}) is:

$$F = 3.2 \times 10^{-4} T_s^{15/4} [\beta/(1-\beta)]^{1/2} . \tag{13}$$

The surface temperature T_s derived by combining equations (7) and (13) is appreciably higher than the effective temperature T_{eff}; the emitted spectrum is therefore harder than that of a simple sum-of-blackbodies.

It is important to note the weak dependence of the temperature T_s on the parameters:

$$T_s \propto M^{-4/15} \beta^{-2/15} .$$

Any change of β will affect the temperature and density profiles (eq. [5]), and the location of the photosphere will vary as well, keeping the temperature T_s almost constant, independently of β (cf. Begelman 1985). The scaling of the viscosity parameter α^* with β ($\alpha^* \propto \beta^{-4}$) is such that the temperature of the photosphere will be very weakly dependent on α^*.

A detailed analysis of the spectral regime can be performed *a posteriori*. Consider first the frequency ν_0 at which the scattering and absorption coefficients are equal: for $x > x_0 = h\nu_0/kT_s$, electron scattering will modify the emission spectrum. For the model considered here it is $x_0 \approx 10^{-2}$, so scattering is indeed important over most of the spectrum. The frequency ν_c for which Compton upscattering of photons becomes important is defined by $y(\nu_c) = 1$, where $y(\nu)$ is the frequency-dependent Compton parameter (Rybicki and Lightman 1979):

$$y(\nu) = 4kT_s \tau_T^2(\nu)/(mc^2) . \tag{14}$$

Here $\tau_T(\nu)$ is the electron scattering optical depth between emission and escape from the medium, so it is measured from an effective absorption optical depth, $\tau_*(\nu)$, of order unity. Comptonization will affect the emerging radiation significantly for $x \geq x_c = h\nu_c/kT_s$; if $x_c \ll 1$, the inverse Compton will go to saturation point and a Wien peak will be produced around $3kT_s$. For the model considered here it is $x_c \geq 1$; thus, inverse Compton scattering may be neglected since the majority of photons undergo coherent scattering.

For an observer at a distance D, the flux at frequency ν from the disk is given by

$$F_\nu = \frac{1}{D^2} \int_\Sigma I_\nu(\boldsymbol{n})(\boldsymbol{n} \cdot \boldsymbol{N}) d\Sigma , \tag{15}$$

where $\boldsymbol{N}$ is the outward normal to the surface area element $d\Sigma = r[1 + (dh/dr)^2]^{1/2} \, dr \, d\varphi$, and $\boldsymbol{n}$ is the direction of the line of sight. We assume that the surface of the disk radiates isotropically, $I_\nu(\boldsymbol{n})$ independent of $\boldsymbol{n}$ for $\boldsymbol{n} \cdot \boldsymbol{N} > 0$.

Let us specify a line of sight in the plane $\varphi = \pi/2$ and denote with ϑ_0 the angle between the line of sight and the rotation axis. Represented in the Cartesian coordinates (X, Y, Z), with the Z-axis being the symmetry axis of the system, the unit vectors can be written as

$$\boldsymbol{n} = \boldsymbol{y} \sin \vartheta_0 + \boldsymbol{z} \cos \vartheta_0 ;$$

$$\boldsymbol{N} = \boldsymbol{x} \sin \vartheta \cos \varphi + \boldsymbol{y} \sin \vartheta \sin \varphi + \boldsymbol{z} \cos \vartheta ,$$

and we have $I_\nu(\boldsymbol{n}) = 0$ for $\boldsymbol{n} \cdot \boldsymbol{N} \leq 0$.

The self-shadowing of the disk must be taken into account. Geometrical thicknesss causes, in fact, occultation of the innermost (and the hottest) regions for high-inclination systems. Consider the element of area at the point $P_0 \equiv (r_0, \pi/2, z_0)$ on the surface of the funnel, whose outward normal $\boldsymbol{N}_0$ is perpendicular to the line of sight, and denote with $\boldsymbol{R}$ the vector connecting P_0 to a generic point $P \equiv (r, \varphi, z)$ on the funnel walls:

$$\boldsymbol{N}_0 = -\boldsymbol{y} \cos \vartheta_0 + \boldsymbol{z} \sin \vartheta_0 ;$$

$$\boldsymbol{R} = \boldsymbol{x} r \cos \varphi + \boldsymbol{y}(r \sin \varphi - r_0) + \boldsymbol{z}(z - z_0) .$$

The condition $\boldsymbol{R} \cdot \boldsymbol{N}_0 = 0$ yields the range of integration over φ in equation (15), which is obviously limited by the eclipsing effect. The observed disk spectrum will then strongly depend on the viewing angle ϑ_0.

The resulting spectrum is shown in Figure 3, where the specific luminosity $4\pi D^2 F_\nu$ (ergs s^{-1} Hz^{-1}) is plotted versus the frequency ν for different inclination angles. As expected from Figures 1 and 2, disks seen more edge-on ($\vartheta_0 \approx 90°$) look cooler and underluminous, the observed bolometric luminosity being only a fraction (about one-tenth) of the total energy output. Since the temperature in the outer parts of the disk is roughly constant, the spectrum is approximately that of a single-temperature modified blackbody. In the model considered here it peaks at $\log \nu \approx 15.3$ (1500 Å) and then falls off exponentially. The temperature of the outer regions, however, does depend on the particular choice of the outer edge of the torus. The logarithmic enhancement of the emitted luminosity with increasing $r_{\rm out}$ (eq. [9]) actually occurs mainly in the inner regions. The luminosity of the outer, spherical body of the torus is always close to about $L_{\rm E}$. The outer temperature then scales as $T_{\rm out} \propto r_{\rm out}^{-1/2}$. However a temperature $T \approx 30{,}000$ K may represent a sort of minimum limiting temperature for the outer, radiation-dominated atmosphere (Blandford 1984). If the effective temperature is reduced below this value, the material opacity changes due to He recombination and the atmosphere cannot remain balanced.

At smaller inclination angles, the funnel region becomes more and more visible. The hottest parts of the disk start contributing to the integrated spectrum, which therefore hardens and flattens at high frequencies, the spectral turnover always occurring between ~ 1500 and 1200 Å. The dependence on the inclination angle of the observed luminosity at a given frequency $\bar{\nu}$ is depicted in Figure 4 for $\log \bar{\nu} = 15.5$, 16, 16.5, and 17. The self-shadowing of the disk has a dramatic effect at the highest frequencies. The curves rise steeply up to the point where the angle ϑ_0 is roughly equal to the funnel opening angle $\psi \approx 23°$ and most of the innermost regions become visible, then flatten at smaller angles. Soft X-ray emission is observed only at inclination angles smaller than ψ, the associated probability $P = 1 - \cos \psi$ being equal to $\sim 8\%$ for the model considered.

In these calculations we have neglected the relativistic effects on the propagation of radiation from the disk, namely the Doppler shift, the gravitational redshift, and the gravitational focusing effect. For a thin disk around a Schwarzschild hole these are minor effects except for an observer near the equator, who sees radiation from the innermost regions to be blueshifted and strongly focused (Cunningham 1975). This

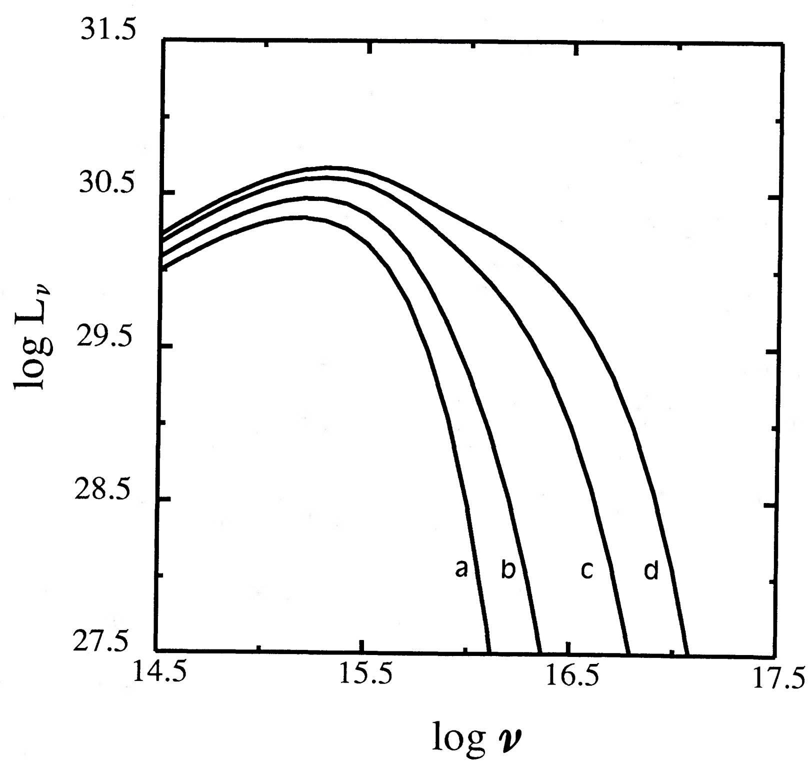

FIG. 3.—Disk spectra for different angles, ϑ_0, of inclination between the rotation axis and the line of sight. Curves labeled a, b, c, and d are computed for $\vartheta_0 = 90°$ (edge-on view), 50°, 25°, and 0° (pole-on view), respectively.

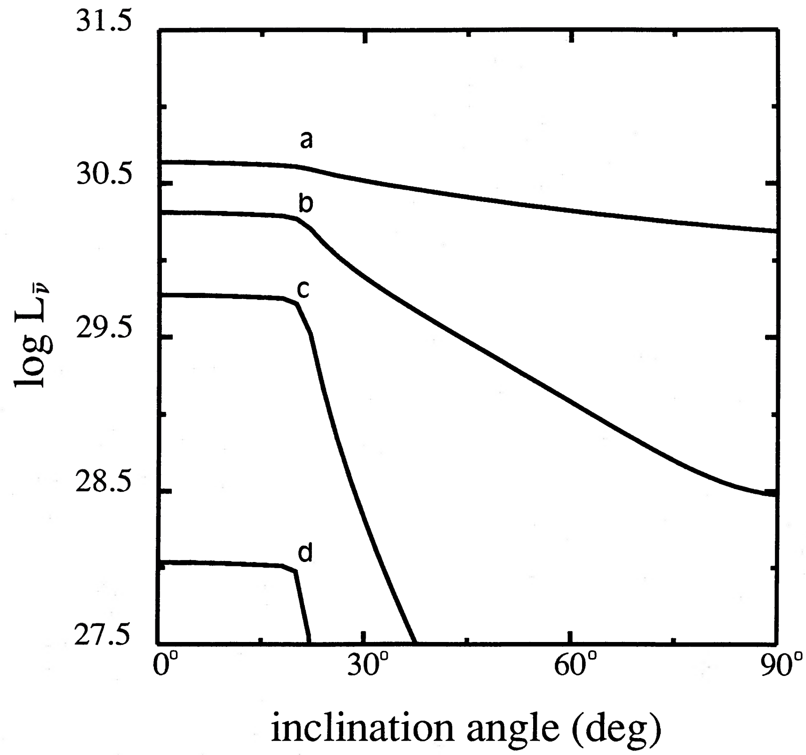

FIG. 4.—Dependence of the observed specific luminosity on the inclination angle. Curves labeled *a*, *b*, *c*, and *d* are computed for log $\bar{\nu}$ = 15.5, 16, 16.5, and 17, respectively. The break in the curves occurs for an angle $\sim 20°$, when most of the funnel becomes visible.

enhancement cannot be directly observed in thick accretion disks because of the strong eclipsing effect at and near the equatorial plane. However, it will affect somewhat the flux of radiation falling on the funnel surface. The problem of scattered radiation will be discussed in detail in the next section.

IV. THE REFLECTION EFFECT

So far mechanical equilibrium between gravity, centrifugal force, and pressure of the outgoing radiation has been assumed. However, when we consider the funnel surface, the incoming radiation from the other parts of the funnel must be included in the balance of forces, the local effective gravity determining in this case the *net* radiative flux perpendicular to the surface (Sikora 1981).

Within the funnel, in fact, each photon will in general scatter many times before escaping either to infinity or falling down into the black hole. As a result of multiple scatterings, the surface brightness will be much larger than the net flux. If the opening solid angle of the funnel is Ω_0, then the surface brightness will be enhanced by a factor $\leq 2\pi/\Omega_0$.

It is then important to include this reflection effect in our calculations, to get the correct angle-averaged radiation luminosity. In the following we will assume an empty funnel in which the radiation is *scattered isotropically* off the surface elements of the disk. This implies that the local thermal state of the emitting material at $\tau_* = 1$ is not modified by the incoming flux. This is a reasonable approximation because we have seen that, in the conditions envisaged, the Thomson opacity dominates at frequencies $x \geq 10^{-2}$; hence, most of the photons are thermalized well below the last scattering surface. Low-energy incoming photons, however, will be absorbed in the upper atmospheric layers, and the local temperature of the emitting gas will increase. A Newtonian approximation will be also used in the following.

The balance of forces normal to the surface is now given by the integral equation:

$$F_e - F_{\rm in}^N = (c/k_T)g_{\rm eff} , \tag{16}$$

where F_e is the sum of the flux which is locally generated and of the flux which is scattered isotropically, and $F_{\rm in}^N$ is the normal component of the incoming flux:

$$F_{\rm in}^N = 1/\pi \int F_e(\boldsymbol{R} \cdot \boldsymbol{N}) d\Omega . \tag{17}$$

Here $d\Omega$ is the element of solid angle associated with the direction $\boldsymbol{R}$ within which the incoming radiation is seen at a given point. It is the integral term which takes into account the radiative interactions between different zones of the funnel.

The distribution of emitted flux F_e has been obtained (see also Sikora 1981) by subdividing the surface of the funnel into a large, finite number of emitting rings and by approximating equation (16) as

$$F_{e,i} - 1/\pi \sum_j B_{ij} F_{e,j} = (c/k_T) g_{{\rm eff},i} . \tag{18}$$

We have then to solve the set of linear algebraic equations which results from equation (18). The elements of the diagonally dominant matrix B_{ij} represent the fraction of the radiation emitted from the jth ring which reaches the ith ring.

Consider the points P_i and $P_j \equiv (r_j, \varphi_j, z_j)$, respectively, on the ith and jth ring and denote with N_i and N_j the outward normal vectors to the surface area elements at those points. We can then write

$$B_{ij} = \int_{\Omega_{ij}} \frac{(N_i \cdot R)}{|R|} d\Omega , \tag{19}$$

where R is the vector connecting P_i to P_j and Ω_{ij} is the solid angle within which an observer located at the ith ring sees the jth ring. The solid angle element is

$$d\Omega = \frac{(N_j \cdot R)}{|R|^3} d\Sigma_j = \frac{(N_j \cdot R)}{|R|^3} r_j \left[1 + \left(\frac{dh}{dr}\right)_j^2\right]^{1/2} d\varphi \, \Delta r , \tag{20}$$

where Δr is the mesh size. A grid of 350 points has been used to approximate equation (16). The integration over φ in equation (19) can be performed analytically using elementary functions. However, self-shadowing of the funnel surface, which again limits the range of integration over φ in equation (19), must be taken into account.

A substantial increase of the surface brightness results, as may be seen in Figure 5 for the model of radiation torus considered above. It is important to stress that the tangential components of the external radiative force are left unbalanced. This will have little effect on the equilibrium structure at large optical depths, but strict hydrostatic equilibrium will not be maintained in a surface layer of thickness $\leq 1/(\rho k_T)$ (Nityananda and Narayan 1982). Upward acceleration of the funnel walls will occur; the outflowing matter will probably carry away, in the optically thin case, a particle luminosity $\leq L_E$ (Narayan, Nityananda, and Wiita 1983).

We have assumed, in fact, that the mass outflow does not make the funnel optically thick and have ignored any modification of the radiation field by the moving walls. To compute how the multiple scatterings of photons modify the spectrum of the disk, equation (18) has to be solved at each frequency, the local specific intensity being given by equation (12).

The resulting spectrum is shown in Figure 6 for different inclination angles; comparison with Figure 3 clearly shows the luminosity enhancement due to multiple reflections. The dependence of the observed specific luminosity on the viewing angle is depicted in Figure 7. The hard photons emitted in the innermost regions of the disk, regions which are shadowed for high inclination angles, will be scattered by the funnel walls into the line of sight. That is why the self-occultation effect at the highest frequencies is less pronounced than in Figure 4. In particular, soft X-ray emission will be observed now at viewing angles which are much larger than ψ, up to $\vartheta_0 \approx 50°$. In this case we should expect to see a much higher fraction of soft X-ray emitting sources, about $\sim 35\%$.

The luminosity emitted per logarithmic frequency interval is plotted in Figure 8 in the case of the face-on view ($\vartheta_0 = 0°$). In the same figure the emission spectra of a thin disk and of a radiation torus without the inclusion of the reflection effect are shown for comparison.

V. DISCUSSION

The nature and the shape of the ultraviolet continuum in quasars are debatable. There is strong evidence that a large fraction of the luminosity emitted by active nuclei is produced in the ultraviolet band, maybe well beyond the Lyman edge. Thermal emission from an accretion disk is an attractive, although not unique, explanation.

Thin accretion disk models are very popular; spectral fits in the simple sum-of-blackbodies approximation have been performed by Malkan (1983), who has interpreted the steepening of the UV continuum shortward of $\lambda \approx 1500$ Å as the exponen-

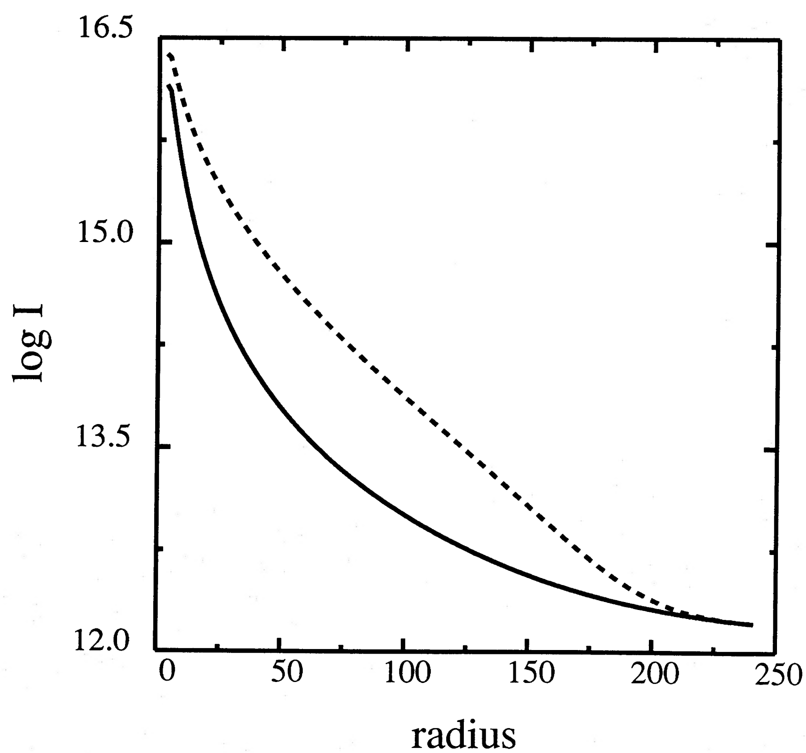

FIG. 5.—The surface brightness (*dashed curve*) and effective gravity or net flux (*solid curve*) vs. radius in the funnel (in units of r_G). Note the enhancement due to the *reflection effect*.

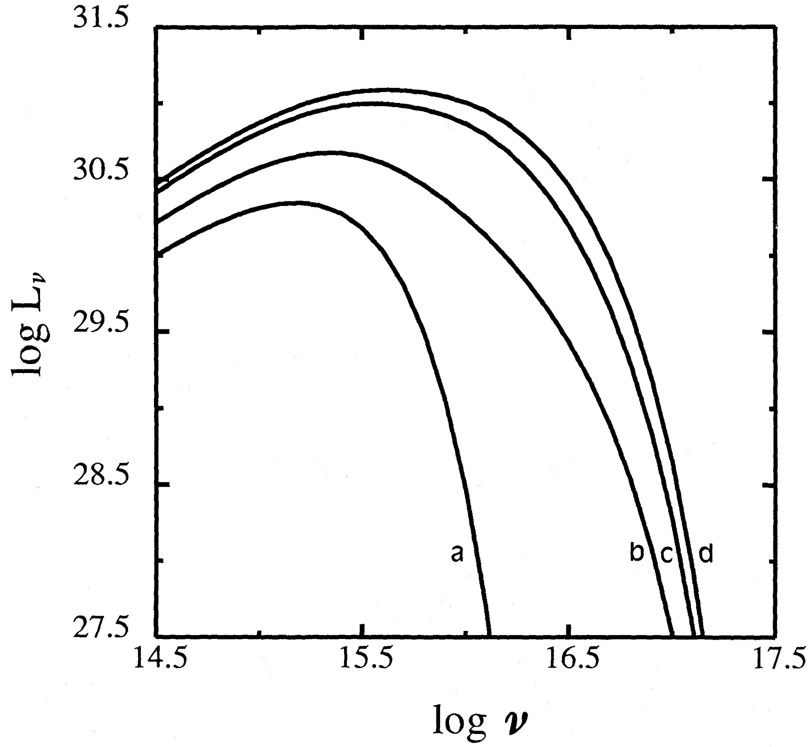

FIG. 6.—Disk spectra for different inclination angles. The effect of multiple scatterings off the funnel walls has been included. Curves labeled *a*, *b*, *c*, and *d* are computed for $\vartheta_0 = 90°, 50°, 25°$, and $0°$, respectively.

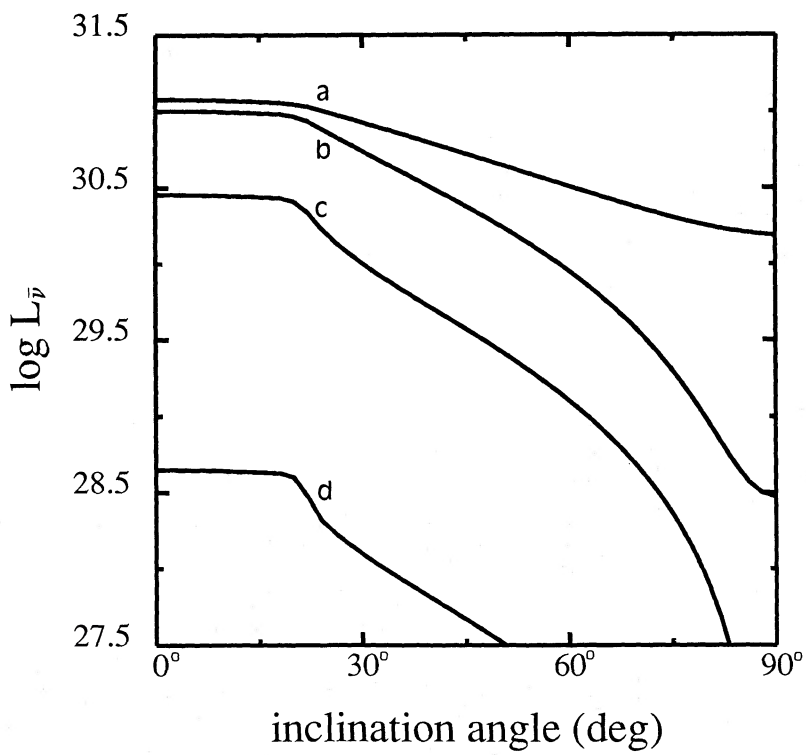

FIG. 7.—Dependence of the observed specific luminosity on the inclination angle. The effect of multiple scatterings off the funnel walls has been included. Curves labeled *a*, *b*, *c*, and *d* are computed for log $\bar{\nu}$ = 15.5, 16. 16.5, and 17, respectively.

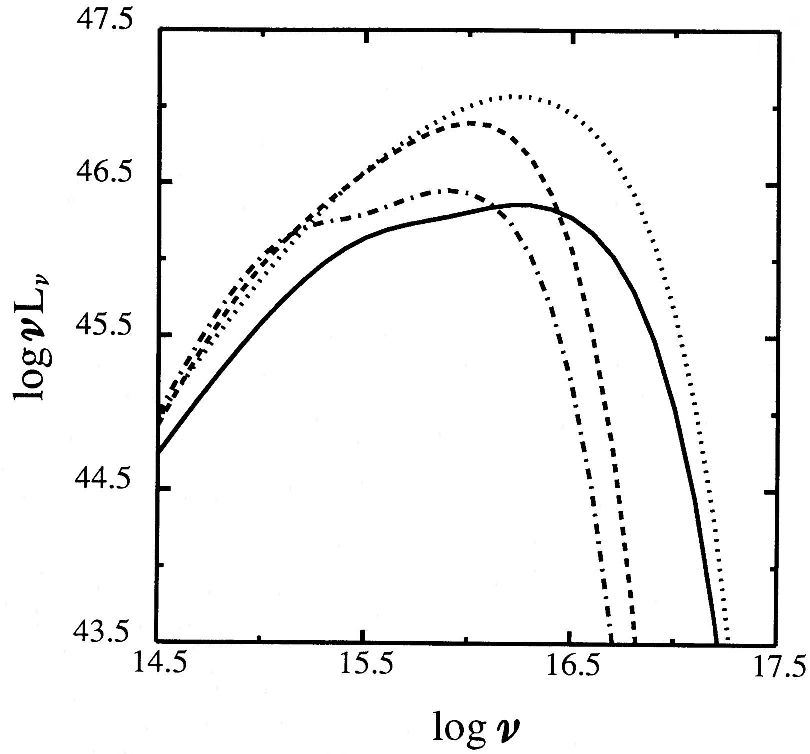

FIG. 8.—Spectra at $\vartheta_0 = 0°$ (pole-on view) replotted in terms of luminosity per logarithmic frequency interval. *Solid line*: thick disk spectrum without reflection effect; *dash-dotted line*: same in the sum-of-blackbody approximation; *dotted line*: thick disk spectrum with reflection effect; and *dashed line*: thin disk spectrum with the same M, $\dot{M}$, and size.

tial cut-off of the thermal spectrum. However, the basic problem with this interpretation is that this portion of the spectrum coincides with the natural scale energy of atomic physics and strong absorption by the gas along the line of sight is likely to occur.

In fact, *IUE* observations of moderate redshift ($1 \leq z \leq 2$) quasars (Bechtold *et al.* 1984) show a redshift-correlated steepening in the continuum at about ~1200 Å, from a power law in the optical $\alpha \approx 0.5$ to $\alpha \approx 3 \div 5$ shortward Lyα. This probably arises from Lyman-continuum absorption by intervening neutral H along the line of sight.

Recent, high-resolution observations of very high z QSOs ($z \geq 2.7$; Steidel and Sargent 1987) indicate that the steepening in the continuum slope shortward Lyα is not intrinsic to the quasar but is due to the effect of blanketing of Lyα, Lyβ, Ly-continuum absorption by a cosmological distribution of intervening, neutral Lyα clouds. This is consistent with the absence of a turnover in $z < 0.5$ objects (Kinney *et al.* 1985). The apparent steepening observed in *IUE* low-resolution spectra would then be completely unrelated to the intrinsic continuum of the hypothetical accretion disk; the inferred blackbody peak temperature $T \approx 30{,}000$ K would be then too low and just reflect the absorption cut-off at Lyα.

In principle, it might be possible to use the observed relative strengths of optical and UV emission lines to infer information about the extreme-UV continuum shape (Krolik and Kallman 1987). The problem with emission-line diagnostics is basically that the ionization parameter is much more important than the exact shape of the ionizing spectrum (provided it extends above the relevant ionization thresholds) in determining the line ratios.

The observed UV spectrum might also be too steep and too faint to produce the total emission-line flux, as pointed out by Netzer (1985). An *energy budget* problem actually arises from standard photoionization models; apparently, the total line emission and Balmer continuum flux is about 8 times the Lyα flux (in case B recombination, the number of Lyα photons escaping the cloud equals the number of ionizing photons absorbed by it). Again, a much flatter intrinsic Lyman continuum ($\alpha < 0.4$) might be required.

Observational determinations of the frequency, where the thermal component peaks, are thus very uncertain. In this respect, the extreme cases of disk spectra extending up to the highest frequencies may be represented by those quasars (such as PG 1211+143, Mkn 335, Mkn 841) with a large excess of soft X-ray emission above the extrapolation of the >2 keV power-law spectrum. This soft X-radiation would be emitted from the innermost parts of the disk, while the optical/UV continuum would originate in the outer, cooler disk regions. The interpretation of this excess as the hot ($T \leq 10^6$ K) tail of the accretion disk spectrum, besides making this UV/X-ray feature dominate the luminosity of the source, requires high super-Eddington accretion rates.

Opacity effects in more realistic thin-disk models have been recently explored by Czerny and Elvis (1987). These effects strongly modify the simple sum-of-blackbodies spectrum, making it harder and so alleviating the super-Eddington problem. These authors explain the observed spectral flattening at ~1500 Å as being due to the onset of electron scattering, and they also discuss the importance of occultation effects. However, these models still require $L \geq L_E$; i.e., they imply an accretion regime in which radiation-supported tori, rather than thin accretion disks, are expected to form.

We were then led to investigate a thick-disk model which depends on the following parameters: the black hole mass M, the angular momentum distribution $l(r)$ (which in turn determines $\dot{M}$), and the ratio of the gas pressure to the total pressure β. We have computed the resulting thermal emission spectrum; opacity effects due to coherent electron scattering have been taken into account. More importantly, the self-shadowing and the multiple reflection effects have been included.

A striking dependence of the spectrum on the viewing angle of the observer is found. Different inclinations result in a range of apparent luminosities and color temperatures, the UV continuum being flatter for increasing luminosities. If the IR power law is a distinct component (as variability data suggest; see Cutri *et al.* 1985) and it is emitted isotropically, the thermal-to-power-law flux ratio increases with the decreasing viewing angle, and an anticorrelation between the optical/UV luminosity and the IR/optical continuum slope is expected. The existence of such a correlation has been recently suggested by Wandel (1987).

Within this model, it is then natural to interpret optical/UV bumps peaking at $\lambda \leq 1500$ Å as due to thermal emission from thick accretion disks seen almost equator-on ($\vartheta_0 \approx 90°$). Soft X-ray emission would be observed at small inclination angles.

As a result of multiple scatterings of photons off the funnel walls, the surface brightness in the funnel is greatly enhanced (Sikora 1981). The distribution of luminosity at infinity is such that, along the rotation axis, the effective luminosity exceeds the Eddington limit by more than a factor of 20, which is 4 times the luminosity averaged over all angles (see Fig. 9). At inclination angles which are smaller than the funnel opening angle ψ, luminosities of order 10^{47} ergs s^{-1} will be observed from thick accretion disks orbiting a black hole of mass only $\sim 5 \times 10^7 M_{\odot}$.

Some of the implications of an anisotropic ionizing continuum for photoionization models of the BLR have been recently discussed by Netzer (1987). Generally speaking, line-emitting clouds at small inclination angles would be subject to a stronger ionization flux and so emit mostly high-excitation lines compared with clouds near the equatorial plane, which would emit mainly low-excitation lines. The angular dependence of the ionization parameter and of the covering factor would be a critical feature of the model. Physical parameters of the BLR could differ crucially from previous standard estimates.

The strong soft X-ray emission observed nearly pole-on could actually inhibit the very formation of clouds near the disk rotation axis. In the standard two-phase instability model (Krolik, McKee, and Tarter 1981) a steep soft X-ray spectrum would not lead to the formation of a two-phase medium, with cold ($\sim 10^4$ K) line-emitting clouds being pressure-confined by a hot ($\sim 10^8$ K) intercloud medium, the hot-phase temperature being determined by the balance of Compton heating and cooling (Guilbert, Fabian, and McCray 1983). Now, if one assumes power-law emission in the X-ray band to be spherically symmetric, cooling dominates heating at small angles and no two-phase medium is formed. A BLR would thus form only at high inclination angles (Fabian *et al.* 1986; Bechtold *et al.* 1987).

Soft X-ray excesses have been observed in radio-quiet, optically bright QSOs. It has already been suggested by Blandford (1984) that in a simplified unified scheme for different types of active galaxies, controlled by the parameters $\dot{m}$–M, radio-quiet QSOs may be identified with supercritical accreting tori. The geometrical effect of the absorption of primary ionizing photons by a toroidal thick configuration has been invoked for radio-quiet QSOs as a possible explanation for the presence of strong nuclear Fe II optical lines (Boroson, Oke, and Persson 1985). Basically, radio-quiet QSOs (and compact flat spectrum

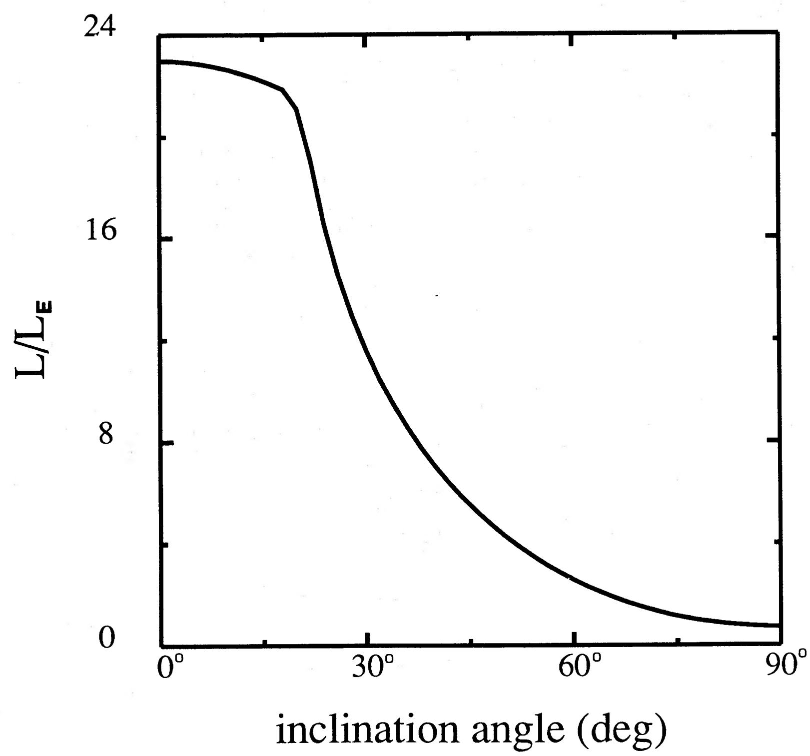

FIG. 9.—The distribution of bolometric luminosity at infinity, as a function of the inclination angle from the rotation axis

objects) have stronger Fe II emission lines than steep-spectrum extended radio quasars.

A possible explanation is that the optically thick torus which we suggest may power the radio-quiet QSOs (and which may produce and collimate a radio-emitting outflow at, say $\dot{m} \gg 100$, in the case of flat-radio sources) shadows the outer, line-emitting material from the inner source of hard, ionizing radiation. The softer ionizing flux observed closer to the equatorial plane would allow a lower ionization stage of the iron, thus increasing the strength of the optical Fe II emission. Subcritical thin accretion disks would instead be characterized by a higher flux of ionizing radiation which can get out into the surrounding material; this would ionize iron and reduce the Fe II emission lines.

If this picture is correct, an obvious test is to check for the presence of strong Fe II emission lines in the spectra of the objects which show a soft X-ray excess.

The idea of a strong and anisotropic far-UV continuum may then have many important consequences. A discussion of such possibilities needs more careful modeling and will be the subject of future work.

I would like to thank M. A. Abramowicz for his advice and supervision. I am also grateful to O. Blaes, B. Czerny, G. Ghisellini, P. Mann, D. Raine, and G. Rybicki for stimulating discussions, and to P. Ghosh for a critical reading of the manuscript.

REFERENCES

Abramowicz, M. A. 1985, *Pub. Astr. Soc. Japan*, **37**, 727.
Abramowicz, M. A., Calvani, M., and Nobili, L. 1980, *Ap. J.*, **242**, 772.
Abramowicz, M. A., Henderson, P. F., and Ghosh, P. 1983, *M.N.R.A.S.*, **203**, 323.
Abramowicz, M. A., and Piran, T. 1980, *Ap. J. (Letters)*, **241**, L7.
Arnaud, K. A., *et al.* 1985, *M.N.R.A.S.*, **217**, 105.
Bechtold, J., Czerny, B., Elvis, M., Fabbiano, G., and Green, R. F. 1987, *Ap. J.*, **314**, 699.
Bechtold, J., Green, R. F., Weymann, R. J., Schmidt, M., Estabrook, F. B., Sherman, R. D., Wahlquist, H. D., and Heckman, T. 1984, *Ap. J.*, **281**, 76.
Begelman, M. 1985, in *Astrophysics of Active Galaxies and Quasi-Stellar Objects*, ed. J. S. Miller (Oxford: Oxford University Press), p. 411.
Blaes, O. M. 1986, Ph.D. thesis, SISSA, Trieste.
———. 1987, *M.N.R.A.S.*, **227**, 975.
Blaes, O. M., and Hawley, J. F. 1987, preprint.
Blandford, R. D. 1984, in *Proc. of the Manchester Conference on Active Galactic Nuclei*, ed. J. Dyson (Manchester: University Press), p. 281.
———. 1985, in *Numerical Astrophysics*, ed. J. Centrella, J. LeBlanc, and R. L. Bowers (Boston: Jones and Bartlett Publishers, Inc.), p. 6.
Boroson, T. A., Persson, S. E., and Oke, J. B. 1985, *Ap. J.*, **293**, 120.
Cunningham, C. T. 1975, *Ap. J.*, **202**, 788.
Cutri, R. M., Wisniewski, W. Z., Rieke, G. H., and Lebofsky, M. J. 1985, *Ap. J.*, **296**, 423.
Czerny, B., and Elvis, M. 1987, *Ap. J.*, **321**, 305.
Elvis, M., Green, R. F., Bechtold, J., Schmidt, M., Neugebauer, G., Soifer, B. T., Mathews, K., and Fabbiano, G. 1986, *Ap. J.*, **310**, 291.
Elvis, M., Wilkes, B. J., and Tananbaum, H. 1985, *Ap. J.*, **292**, 357.
Fabian, A. C., Guilbert, P. W., Arnaud, K. A., Shafer, R. A., Tennant, A. F., and Ward, M. J. 1986, *M.N.R.A.S.*, **218**, 457.
Frank, J. 1979, *M.N.R.A.S.*, **187**, 883.
Goldreich, P., Goodman, J., and Narayan, R. 1986, *M.N.R.A.S.*, **221**, 339.
Gondhalekar, P. M., O'Brien, P., and Wilson, R. 1986, *M.N.R.A.S.*, **222**, 71.
Guilbert, P. W., Fabian, A. C., and McCray, R. 1983, *Ap. J.*, **266**, 466.
Jaroszynski, M., Abramowicz, M. A., and Paczyński, B. 1980, *Acta Astr.*, **30**, 1.
Kinney, A. L., Huggins, P. J., Bregman, J. N., and Glassgold, A. E. 1985, *Ap. J.*, **291**, 128.
Kozlowski, M., Jaroszynski, M., and Abramowicz, M. A. 1978, *Astr. Ap.*, **63**, 209.
Krolik, J. H., and Kallman, T. R. 1987, *Ap. J. (Letters)*, **320**, L5.
Krolik, J. H., McKee, C. F., and Tarter, C. B. 1981, *Ap. J.*, **249**, 422.
Malkan, M. A. 1983, *Ap. J.*, **268**, 582.
Malkan, M. A., and Sargent, W. L. W. 1982, *Ap. J.*, **254**, 22.
Maraschi, L., Reina, C., and Treves, A. 1976, *Ap. J.*, **206**, 295.
Narayan, R., Nityananda, R., and Wiita, P. J. 1983, *M.N.R.A.S.*, **205**, 1103.
Netzer, H. 1985, *Ap. J.*, **289**, 451.
———. 1987, *M.N.R.A.S.*, **225**, 55.
Neugebauer, G., Oke, J. B., Becklin, E. E., and Matthews, K. 1979, *Ap. J.*, **230**, 79.
Nityananda, R., and Narayan, R. 1982, *M.N.R.A.S.*, **201**, 697.
Paczyński, B. 1978, *Acta Astr.*, **28**, 91.
Paczyński, B., and Wiita, P. J. 1980, *Astr. Ap.*, **88**, 23.
Papaloizou, J. C. B., and Pringle, J. E. 1984, *M.N.R.A.S.*, **208**, 721.
———. 1985, *M.N.R.A.S.*, **213**, 799.
Pounds, K. A., Stanger, V. J., Turner, T. J., King, A. R., and Czerny, B. 1987, *M.N.R.A.S.*, **224**, 443.
Pringle, J. E. 1981, *Ann. Rev. Astr. Ap.*, **19**, 137.
Rees, M. J. 1984, *Ann. Rev. Astr. Ap.*, **22**, 471.
Richstone, D. O., and Schmidt, M. 1980, *Ap. J.*, **235**, 377.
Rybicki, G. B., and Lightman, A. P. 1979, *Radiative Processes in Astrophysics* (New York: Wiley).
Shakura, N. I., and Sunyaev, R. A. 1973, *Astr. Ap.*, **24**, 337.
Shields, G. A. 1978, *Nature*, **272**, 706.
Sikora, M. 1981, *M.N.R.A.S.*, **196**, 257.
Singh, K. P., Garmire, G. P., and Nousek, J. 1985, *Ap. J.*, **297**, 633.
Steidel, C. C., and Sargent, W. L. W. 1987, *Ap. J.*, **313**, 171.
Wandel, A. 1987, *Ap. J. (Letters)*, **316**, L55.
Wiita, P. J. 1982, *Ap. J.*, **256**, 666.
Zurek, W. H., and Benz, W. 1986, *Ap. J.*, **308**, 123.

PIERO MADAU: Theoretical Astrophysics, 130–33 California Institute of Technology, Pasadena, CA 91125